



OPEN

## Cysteic acid grafted to magnetic graphene oxide as a promising recoverable solid acid catalyst for the synthesis of diverse 4*H*-chromene

Firouz Matloubi Moghaddam<sup>✉</sup>, Mohammad Eslami & Golfamsadat Hoda

*4H*-chromenes play a significant role in natural and pharmacological products. Despite continuous advances in the synthesis methodology of these compounds, there is still a lack of a green and efficient method. In this study, we have designed cysteic acid chemically attached to magnetic graphene oxide (MNPs-GO-CysA) as an efficient and reusable solid acid catalyst to synthesize *4H*-chromene skeletons via a one-pot three components reaction of an enolizable compound, malononitrile, an aldehyde or isatin, and a mixture of water–ethanol as a green solvent. This new heterogeneous catalyst provides desired products with a good to excellent yield, short time, and mild condition. This procedure presents an environmentally friendly approach for the synthesis of a great number of *4H*-chromene derivatives.

*4H*-chromenes represent an important class of oxygen-containing heterocycles and a key building block of many natural products. They are also widely found in nature, in some edible fruits and vegetables, to name but a few, and these compounds also are broadly used as cosmetics and pigments<sup>1–3</sup>. *4H*-chromene scaffolds exhibit pharmacological properties and biological activities such as antioxidant<sup>4</sup>, antimicrobial<sup>5,6</sup>, antiviral, antibacterial, pro-apoptotic<sup>7–11</sup>, anticancer<sup>12</sup>, antifungal, anticoagulant, antinociceptive<sup>13</sup>, antiproliferative<sup>14</sup>, antitubercular, antiallergic, antibiotic, hypolipidemic, and immunomodulating activities. They also are used as cognitive enhancers, in order to treat neurodegenerative disease<sup>15,16</sup> such as Alzheimer's disease, Huntington's disease, amyotrophic lateral sclerosis, AIDS, Parkinson's disease, Down's syndrome, and also myoclonus and schizophrenia<sup>17</sup>. For example, *4H*-chromene derivatives such as A, B, C, D, and E are known as apoptosis inducer, insulin-regulated aminopeptidase for enhancing memory, learning functions inhibitor, and anticancer therapeutic agents respectively, which are shown in Fig. 1<sup>11,18–20</sup>.

In this regard, multi-component reactions (MCRs) have gained considerable attention for constructing a broad range of complex molecules in a highly efficient, rapid, step-economic, low-cost, and eco-friendly manner<sup>21–27</sup>. Because of the benefits of MCRs and the great importance of *4H*-chromenes, syntheses of these compounds have been developed using different catalysts in the multicomponent reaction between malononitrile (or ethyl cyanoacetate), a diverse electron-rich phenol or enolizable carbonyl compound, and an aldehyde<sup>1</sup>. Recent catalytic systems for the synthesis of *4H*-chromene derivatives consist of Fe(HSO<sub>4</sub>)<sub>3</sub><sup>28</sup>, nickel nanoparticles<sup>29</sup>, ZrO<sub>2</sub> nanoparticles<sup>30</sup>, Zn<sub>4</sub>O(H<sub>2</sub>N-TA)<sub>3</sub><sup>31</sup>, ZnS nanoparticles<sup>32</sup>, nano-sized MgO<sup>33</sup>, CoFe<sub>2</sub>O<sub>4</sub><sup>34</sup>, CuO-CeO<sub>2</sub><sup>35</sup>, egg shell<sup>36</sup>, chitosan<sup>37</sup>, polymer-supported palladacycles<sup>38</sup>, [2-aemim][PF<sub>6</sub>]<sup>39</sup> and TMG-[bmim][X]<sup>40</sup> under microwave radiation, [bmim]OH<sup>41</sup>, IL-HSO<sub>4</sub>@SBA-15<sup>42</sup>, hexadecyltrimethylammonium bromide<sup>43</sup>, L-proline<sup>44</sup>, L-proline-melamine<sup>45</sup>, tetraalkylammonium halides<sup>46–49</sup>, SB-DBU.Cl<sup>50</sup>, potassiumphthalimide-*N*-oxyl<sup>51</sup>, potassium phthalimide<sup>52</sup>, sodium selenate<sup>53</sup>, sodium alginate<sup>54</sup>, Sodium ethylene diamine tetraacetate<sup>55</sup>, morpholine<sup>56</sup>, 4-dimethylamino-pyridine<sup>57</sup>, 4-DMAP<sup>58</sup>, piperidine<sup>18,59</sup>, piperidinium acetate<sup>60</sup>, (DHQD)<sub>2</sub>PYR<sup>61</sup>, tungstic acid functionalized mesoporous SBA-15<sup>62</sup>, 1,8-diazabicyclo[5.4.0]undec-7-ene<sup>63</sup>, glycine<sup>64</sup>, imidazole<sup>65</sup>, heteropolyacid<sup>66</sup>, meglumine<sup>67</sup>, Mg/Al hydrotalcite<sup>68</sup>, PEI@Si-MNP<sup>69</sup>, PEG-SO<sub>3</sub>H<sup>70</sup>, alumina<sup>71</sup>, nano-sized zeolite clinoptilolite<sup>72</sup>, Nickel Nanoparticles<sup>29</sup>, (CTA)<sub>3</sub>[SiW<sub>12</sub>]-Li<sup>+</sup>-MMT<sup>73</sup>, PMO-ICS<sup>74</sup>,

Laboratory of Organic Synthesis and Natural Products, Department of Chemistry, Sharif University of Technology, Azadi Street, P.O. Box 111559516, Tehran, Iran. ✉email: matloubi@sharif.edu

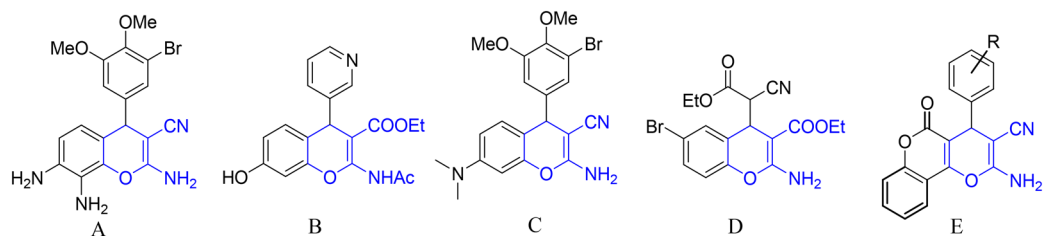


**Figure 1.** Structures of some 4*H*-chromenes possessing diverse biological activities.

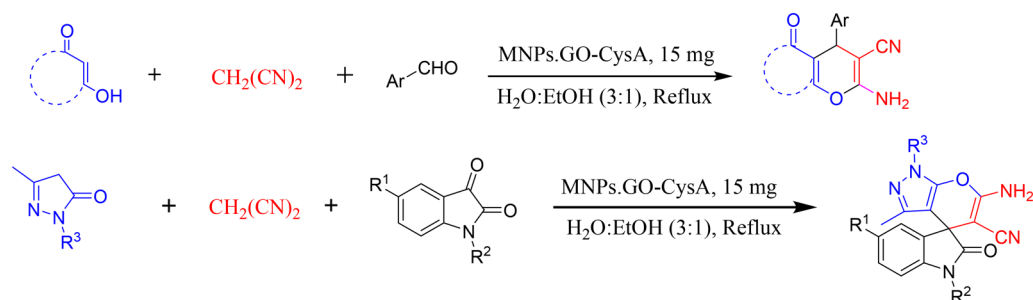


**Figure 2.** One-pot three-component reaction of enolizable compound, active methylene nitriles, and aldehydes catalyzed by MNPs-GO-CysA in water:ethanole.

poly(*N,N'*-dibromo-Nethyl-benzene-1,3-disulfonamide (PBBS)<sup>75</sup>, KSF<sup>76</sup>, combined NaOAc/KF<sup>77</sup>, MeSO<sub>3</sub>H<sup>78</sup>, TiCl<sub>4</sub><sup>79,80</sup>, protic ionic liquid<sup>81</sup>, Bmim(OH)/20 mol% chitosan<sup>82</sup>, MA liquid-phase<sup>83</sup>, Bovine Serum Albumin<sup>84</sup>, and KF alumina<sup>85</sup>.

However, lots of the mentioned catalysts suffer from disadvantages such as environmental pollution, high cost, the difficulty of catalyst removal, and demanding harsh reaction conditions. According to the importance and the broad application of these types of heterocyclic compounds, there is still a great demand for a more feasible, easy, green, and efficient way to synthesize these compounds.

Catalysis is a key to the green chemistry gates. In this regard, the designation of a benign, reusable, and efficient catalyst can provide us with a green approach. Magnetic nanoparticles (MNPs), due to their good dispersion and ease of separation, can be considered as great applicable catalysts in both lab and industrial scales<sup>86,87</sup>. In this study, we designed a magnetic nano-scaled catalyst which has been functionalized by cysteic acid to improve the catalytic activity. By introducing such a catalyst, we can take advantage of both functional groups of graphene oxide and sulfone groups, the broad surface of graphene structure, and ease of separation of a magnetic catalyst.

One of the technical difficulties of typical catalysts is the separation of catalyst off the reaction batch after product gaining. Separation techniques such as filtration and centrifugation are used in such catalysts while magnetic nanoparticles are clearly much more convenient to separate because of their response to an external magnetic field. Using MNPs as catalyst provides the reaction with an effective and rapid way of catalyst separation, making the technique efficiently applicable to both industrial and lab-scale syntheses<sup>88–90</sup>.

To sum up, Graphene Oxide (GO) is the product of chemical exfoliation of graphite, which is an oxygenated monolayer graphene platelet. It contains plentiful of functional groups including hydroxyl, carboxyl, epoxy, and carbonyl group<sup>91</sup>. As a result of having mentioned functional groups, graphene Oxide with its open  $\pi$ -electron system can be easily functionalized by appropriate organic or inorganic molecules. Additionally, GO's 2D structure provides the catalyst system with a high surface area and an excellent mechanical strength<sup>92–96</sup>. Due to the increasing demand for environmentally friendly synthetic processes, using heterogeneous catalysts is getting importance<sup>97–104</sup>. L-cysteic acid, which is an amino acid with a C-terminal sulfonic acid group, can be effectively used as a solid acid catalyst. By magnetizing Graphene Oxide and functionalizing it via an environmentally friendly, bio-degradable Lewis acid, we herein present a new heterogeneous, efficient, easily separable, with a high effective surface available catalyst for synthesizing 4*H*-chromene derivatives (Fig. 2). In general, we took advantage of cysteic acid and graphene oxide as active sites of the catalyst and immobilized these sites on nano-magnetic Fe<sub>3</sub>O<sub>4</sub>, which are bind together via a covalent bond<sup>105,106</sup>.

## Results and discussion

The MNPs-GO-CysA catalyst was synthesized using a few steps presented in Fig. 3. Details of the preparation method are described in the experimental section.

The FTIR spectrum is shown in Fig. 4, demonstrates the formation of desired bonds and the presence of new functional groups of MNPs-GO-CysA. The band at 640 cm<sup>-1</sup> is attributed to the Fe–O bond vibration as proof of the existence of Fe<sub>3</sub>O<sub>4</sub> in MNPs-GO-CysA<sup>107</sup>. The intense broad bands at 3400 can be attributed to stretching of

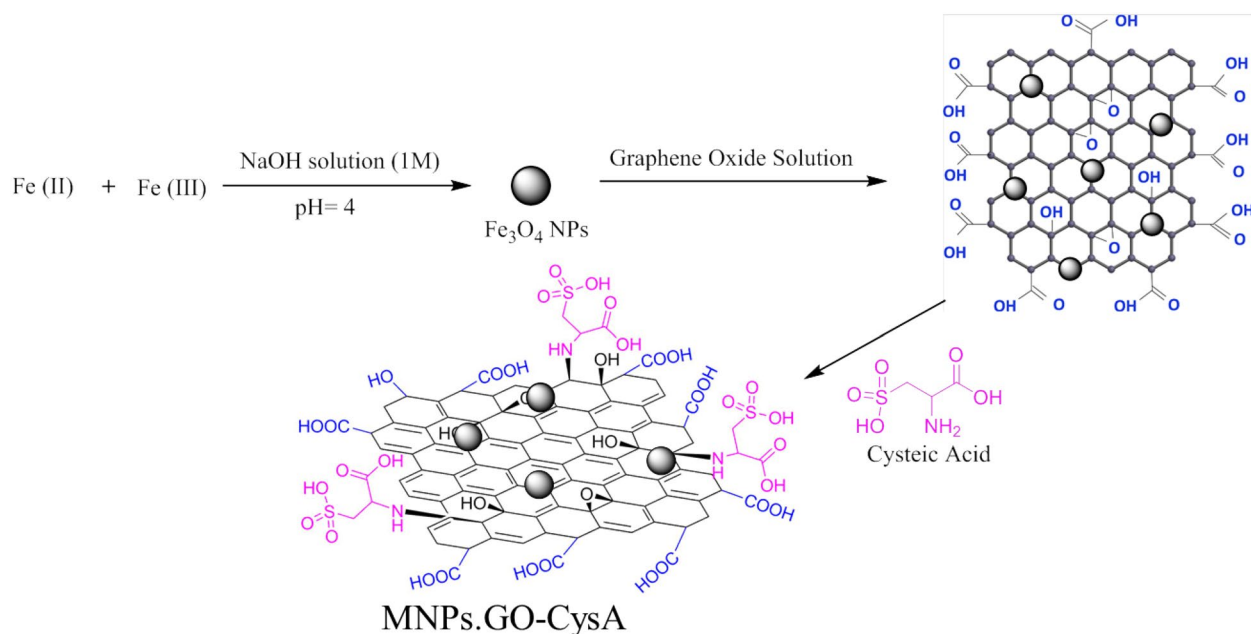


**Figure 3.** The schematic pathway for synthesis of MNPs-GO-CysA.

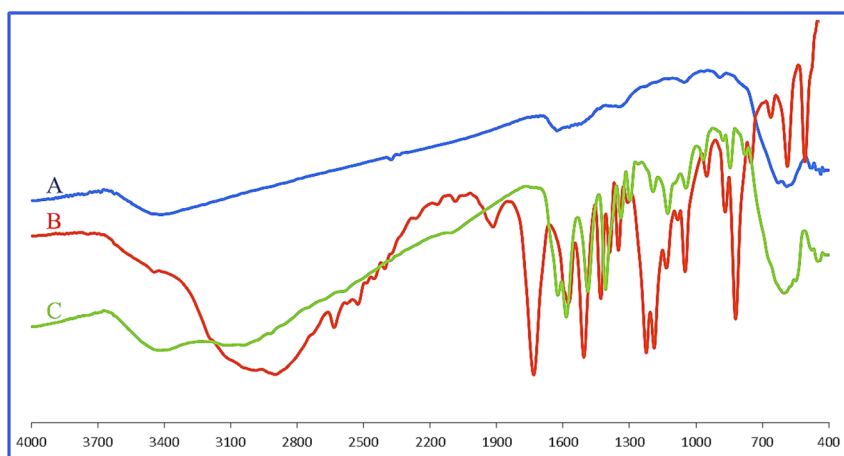


**Figure 4.** The FTIR spectrums of (A)  $\text{Fe}_3\text{O}_4$ , (B) Cysteic acid, and (C) MNPs-GO-CysA.

O–H in GO,  $\text{Fe}_3\text{O}_4$ , and the sulfonic group of cysteic acid<sup>108</sup>. The peaks that appeared at  $1137\text{ cm}^{-1}$  and  $1026\text{ cm}^{-1}$  are due to the  $\text{SO}_2$  asymmetrical and symmetrical stretching vibrations<sup>109</sup>. In addition to the previous note, the absorption peak at  $854\text{ cm}^{-1}$  correspondings to bonded N–H stretching, confirmed the formation of a chemical bond between cysteic acid and the magnetic GO sheets (Fig. 4).

XRD analysis of MNPs-GO-CysA clearly indicates the  $\text{Fe}_3\text{O}_4$  spinel structure (Fig. 5). Peaks located at  $18.95^\circ$ ,  $28.53^\circ$ ,  $30.19^\circ$ ,  $34.40^\circ$ ,  $35.67^\circ$ ,  $43.24^\circ$ ,  $53.63^\circ$ ,  $57.28^\circ$ ,  $62.93^\circ$ , and  $74.54^\circ$  proved the crystallographic structure of  $\text{Fe}_3\text{O}_4$  in the catalyst. Considering the obtained data, the catalyst particles' size was determined to be 10.4 nm from Scherrer's equation based on the most intense peak of  $2\theta = 35.67^\circ$ .

In order to evaluate the structure, morphology, and size of the catalyst, SEM, TEM and EDX analysis were collected. As can be seen in Fig. 6a, the microstructure of MNPs-GO-CysA presented the average size of 16 nm. The TEM micrograph of MNPs-GO-CysA catalyst is shown in Fig. 6b, as shown in Fig. 6b, the sizes of the magnetic  $\text{Fe}_3\text{O}_4$  nanoparticles with tiny particles possessing the spherical morphology were obtained from 10 to 15 nm on a lighter shaded substrate corresponding to the GO sheet. The TEM image of the catalyst (MNPs-GO-CysA) also confirmed that the  $\text{Fe}_3\text{O}_4$  nanoparticles were attached to the surface of graphene oxide free from aggregation. Furthermore, the EDX pattern of the catalyst (Fig. 6c) turned out that MNPs-GO-CysA contains Fe, O, C, N, and S.

CHNS elemental analysis was performed and the results proved the presence of Sulfur atoms in the structure with a scale of 6.68%. The percentage of Sulfur atom in the sample of magnetic GO before the addition of Cysteic acid was determined to be 0.009%. It also appeared that MNPs-GO-CysA contains 1.56% Nitrogen. These results confirm that cysteic acid is successfully attached to the magnetic GO ( $\sim 1.37\text{ mmol g}^{-1}$ ).

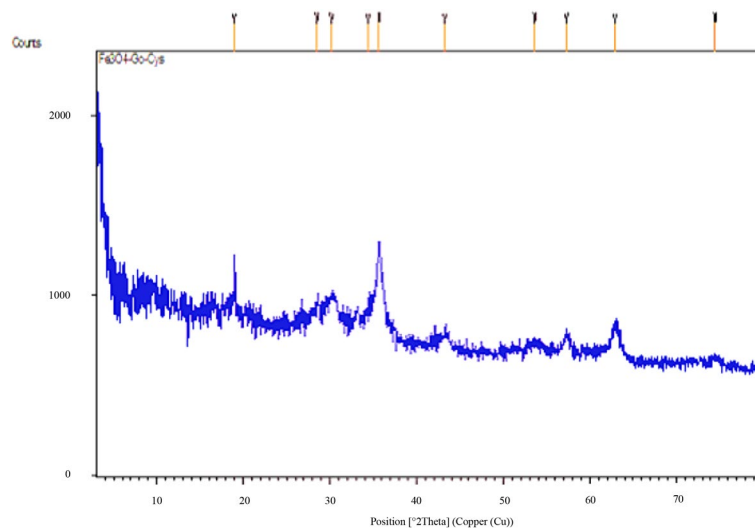


**Figure 5.** XRD pattern of MNPs-GO-CysA.

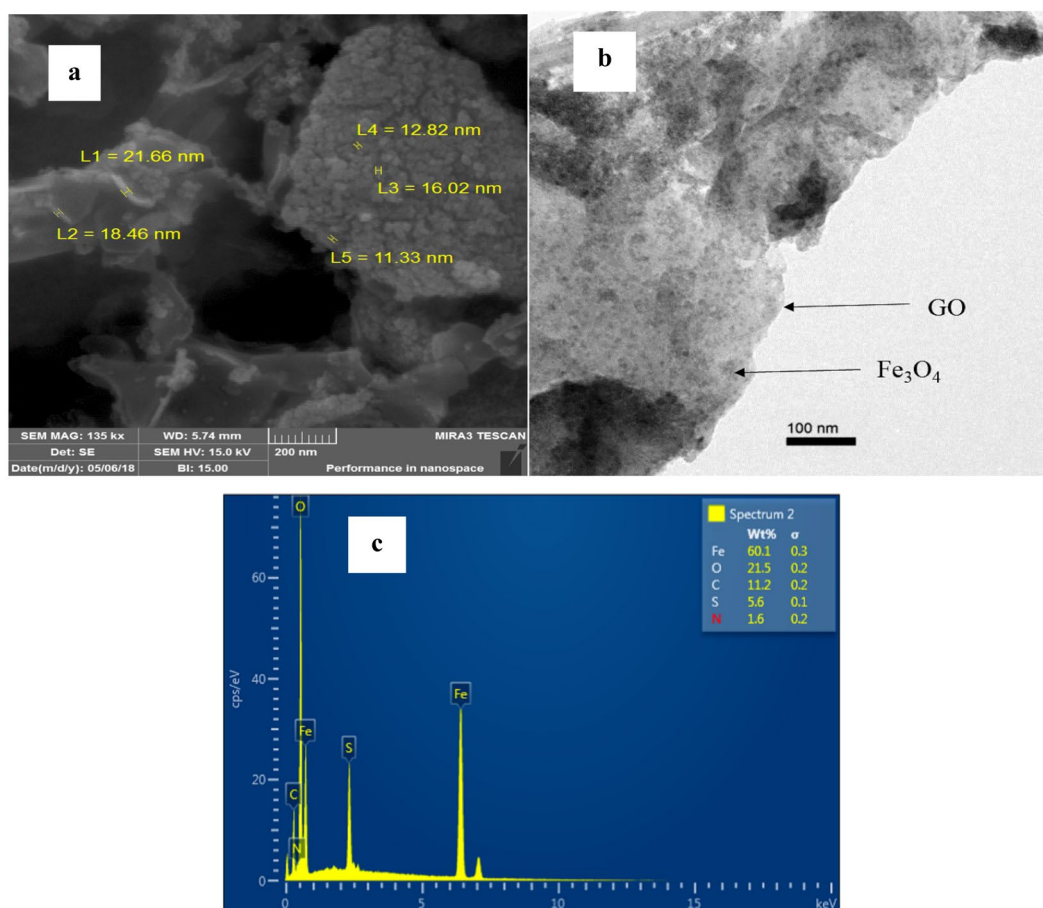


**Figure 6.** (a) SEM, (b) TEM, (c) EDX analyses of MNPs-GO-CysA.

TG-DTG thermograms explain the thermal stability of the MNPs-GO-CysA nanocomposite. All the results derived from TGA analysis are shown in Fig. 7. The first stage of decomposition observed below 180 °C is attributed to physically and chemically trapped water between magnetic GO nanosheets. The second stage of the weight loss, which counted 11.24% between 180 and 220 °C, can be ascribed to the attached organic groups (Cysteic acid) on the surface of magnetic GO nanosheets. Such a relatively high grafting yield suggests successful

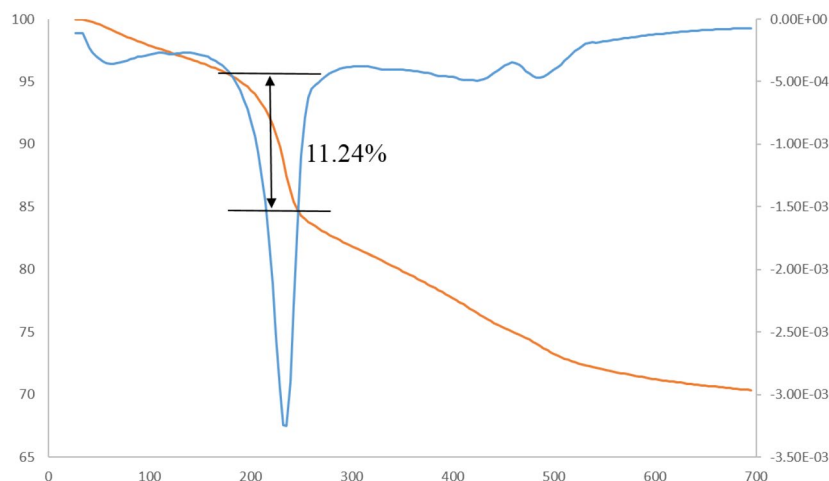


**Figure 7.** TG-DTG thermograms of MNPs-GO-CysA nanocomposite.

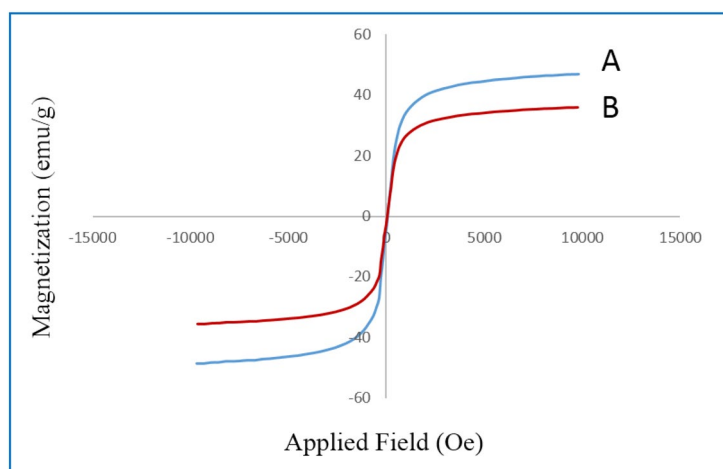


**Figure 8.** S-like curve VSM measurements of  $\text{Fe}_3\text{O}_4/\text{GO}$  (A) and the MNPs-GO-CysA (B) nanocomposites.

attachment of Cysteic acid to  $\text{Fe}_3\text{O}_4/\text{GO}$  surface. The last stage weight loss between 220–600 °C related to the decomposition of graphene oxide nanosheets (the removal of epoxide, hydroxyl, and carboxylic acid surface groups of GO) were performed at the beginning of this stage.

In the next section, the magnetic behavior of the Magnetic graphene oxide functionalized with cysteic acid nanocomposite has been investigated. In this respect, vibrating sample magnetometer (VSM) measurements were carried out at room temperature for both the  $\text{Fe}_3\text{O}_4/\text{GO}$  and the MNPs-GO-CysA nanocomposites. The results shown in the Fig. 8. indicated that the magnetization value of  $\text{Fe}_3\text{O}_4/\text{GO}$  (Fig. 8A) and MNPs-GO-CysA (Fig. 8B) nanocomposites with the S-like curve decreases from 46.83 to 35.25  $\text{emu g}^{-1}$ . This can be attributed to the cysteic acid attached to the  $\text{Fe}_3\text{O}_4/\text{GO}$ .

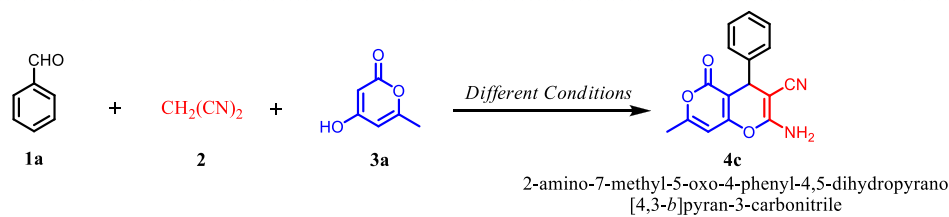
Finally, the activity of the magnetically separable acid catalyst was consequently investigated upon characterization in the diver's derivatives of 4*H*-chromen synthesis. In this regard, to obtain the optimum condition, the three-component reaction between benzaldehyde (1), malononitrile (2), and 4-hydroxy-6-methyl-2*H*-pyran-2-one (3) (molar ratio 1.0:1.1:1.0) was selected as the model reaction and studied in different conditions. The results are summarized in Table 1. In the first step, the reaction was carried out in different solvents including ethanol, water, water-ethanol (3:1), acetonitrile, THF, and solvent-free without any catalysts. The best yield (29%) was obtained in water-ethanol (3:1) in 3 h at room temperature (Table 1, entries 1–6). The Knoevenagel condensation product was formed in quantitative yield as a result of the reaction between benzaldehyde and malononitrile. This result shows that the presence of a catalyst is necessary to improve the desired reaction rate and yield.

In the studies of different green catalysts such as ethylenediaminetetraacetic acid (EDTA), cysteic acid, graphene oxide, and  $\text{Fe}_3\text{O}_4$  nanoparticles on the model reaction, it was found that the best yield of desired product 5e (43%) was obtained when the cysteic acid was used as the catalyst in ethanol-water under reflux conditions (Table 1, entry 7–10).

Studies showed that acidic reagent plays the main role in the catalytic cycle in these reactions. Therefore, cysteic acid was attached as a green biodegradable amino acid to the magnetic graphene oxide to increase the

Entry	Cat. (mg)	Temp	Solv	Time	Yield <sup>b</sup> (%)
1	–	Reflux	EtOH	3 h	14
2	–	Reflux	H <sub>2</sub> O	3 h	16
3	–	Reflux	H <sub>2</sub> O:EtOH (3:1)	3 h	19
4	–	Reflux	CH <sub>3</sub> CN	3 h	Trace
5	–	Reflux	THF	3 h	Trace
6	–	80	Solvent-free	3 h	Trace
7	EDTA 2 mg	Reflux	H <sub>2</sub> O:EtOH (3:1)	3 h	31
8	Cysteic Acid 2 mg	Reflux	H <sub>2</sub> O:EtOH (3:1)	3 h	43
9	GO NPs 2 mg	Reflux	H <sub>2</sub> O:EtOH (3:1)	3 h	27
10	Fe <sub>3</sub> O <sub>4</sub> NPs 2 mg	reflux	H <sub>2</sub> O:EtOH (3:1)	3 h	23
11	MNPs-Go-CysA 5 mg	Ambient	Solvent-free	3 h	43
12	MNPs-Go-CysA 5 mg	80	Solvent-free	3 h	57
13	MNPs-Go-CysA 5 mg	Ambient	Grinding	3 h	40
14	MNPs-Go-CysA 5 mg	REFLUX	H <sub>2</sub> O:EtOH (3:1)	1.5 h	68
15	MNPs-Go-CysA 7.5 mg	REFLUX	H <sub>2</sub> O:EtOH (3:1)	1.5 h	75
16	MNPs-Go-CysA 10 mg	REFLUX	H <sub>2</sub> O:EtOH (3:1)	1.5 h	79
17	MNPs-Go-CysA 12.5 mg	REFLUX	H <sub>2</sub> O:EtOH (3:1)	1 h	82
18	MNPs-Go-CysA 15 mg	REFLUX	H <sub>2</sub> O:EtOH (3:1)	30 min	92

**Table 1.** Optimization of the reaction condition for synthesis of 2-amino-3-cyano-4*H*-chromene catalyzed by MNPs-Go-CysA nanocomposite<sup>a</sup>.



<sup>a</sup>Reaction conditions: Benzaldehyd (1a, 1 mmol), malononitrile (2, 1.1 mmol), and 4-hydroxy-6-methyl-2*H*-pyran-2-one (3a, 1 mmol) in the presence of MNPs-Go-CysA nanocomposite and 2 ml of water–ethanol (3:1) as a green solvent. <sup>b</sup>Isolated Yields.

acidic sites of graphene oxide and to obtain a suitable catalytic activity. Then, the prepared catalyst was used in the model reaction. The reaction was studied under different conditions including running the model reaction at r.t., at 80 °C and using the grinding technique under the solvent-free condition. The desired product was not formed in a suitable yield at any of the mentioned conditions. Interestingly, the product was obtained properly under reflux in water–ethanol (1:3) in the presence of 5 mg of MNPs-Go-CysA nano-catalyst with a yield of 68% after 3 h (Table 1, entries 11–14). Therefore, the effect of catalyst loading on the completion of the reaction was examined in the next experiments (Table 1, entries 15–18). By increasing the catalyst amount from 5 to 15 mg, the reaction yield improved from 68 to 92% at 30 min.

This result clearly shows that the catalyst is effective enough to improve the reaction yield. The active sites of the magnetic nano-catalyst, as a solid acid, can be the acidic functional groups, including the graphene oxide's carboxylic acid group, and the cysteic acid's carboxylic and sulphonic acid groups. These active sites as Bronsted acids improve the reaction yield. The Fe<sub>3</sub>O<sub>4</sub> nano-particles also can race the reaction up as Lewis acids. However, the optimization results indicate the major active site of the nano-particles to be cysteic acid's functional groups.

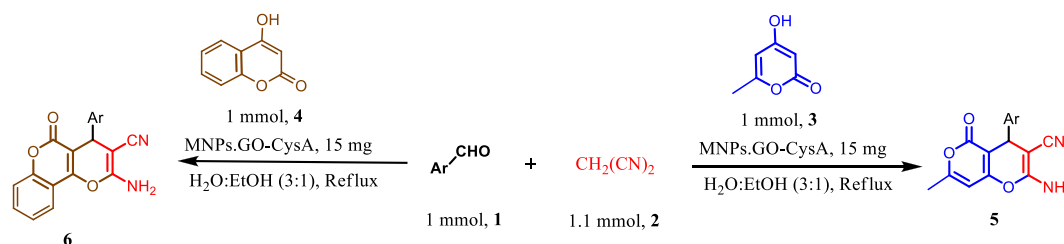
Consequently, we developed the optimized reaction condition (15 mg of MNPs-Go-CysA in 2 ml of water–ethanol (3:1) under reflux conditions) for other derivatives of aromatic aldehydes (1) and enolizable compound (3, 4, 7, 10) for the synthesis of the various derivatives of 2-amino-3-cyano-4*H*-chromenes (5a–j, 6a–j, 8a–j, 11a–l). The results have been presented in Tables 2, 3, 4.

In the next step, to demonstrate the scope of the present protocol, the optimized reaction conditions were examined for Dimedone 7. Dimedone as a cyclic 1,3-dicetone compounds (p*K*<sub>a</sub> = 5.23) required shorter reaction time compared to the 4-hydroxy-pyran and 4-hydroxy-cumarin for the synthesis of 2-amino-7,7-dimethyl-5-oxo-4-aryl-5,6,7,8-tetrahydro-4*H*-chromene-3-carbonitrile (8a–j) in good to excellent yields.

It is noteworthy that in all processes of 2-amino-3-cyano-4*H*-chromene derivatives (5, 6, 8) syntheses, the reaction of aromatic aldehydes which possessed electron-withdrawing groups are shown to be faster than the reaction of aromatic aldehydes with electron-donating groups. Additionally, the reaction was proceeding with heterocyclic aldehydes, and the desired products were obtained in good yields.

En	Aldehyde	Enolizable compound	Product <sup>b</sup>	Time (min)	Yield <sup>c</sup> (%)	M.P. (°C) Obsd./Lit
1	4-Chlorobenzaldehyde	3	5a	15	96	228–230/232 <sup>91</sup>
2	2-Chlorobenzaldehyde	3	5b	25	93	268–269/266–268 <sup>55</sup>
3	4-Nitrobenzaldehyde	3	5c	15	94	213–215/210–212 <sup>55</sup>
4	3-Nitrobenzaldehyde	3	5d	20	95	233–234/234–236 <sup>59</sup>
5	Benzaldehyde	3	5e	30	92	230–232/235–237 <sup>73</sup>
6	Terephthaldehyde	3	5f	45	89	253–255/256 <sup>39</sup>
7	4-Ethoxybenzaldehyde	3	5g	35	93	201–203/224–226 <sup>55</sup>
8	4-Methoxybenzaldehyde	3	5h	30	91	214–216/209–211 <sup>73</sup>
9	3-Methylbenzaldehyde	3	5i	50	89	232–234/235–237 <sup>73</sup>
10	Thiophen-2-carbaldehyde	3	5j	40	91	245–247/240–243 <sup>110</sup>
11	4-Chlorobenzaldehyde	4	6a	20	98	256–257/258–260 <sup>111</sup>
12	2,4-dichlorobenzaldehyde	4	6b	35	89	262–264/258–260 <sup>112</sup>
13	4-Nitrobenzaldehyde	4	6c	14	91	254–256/251–253 <sup>73</sup>
14	3-Nitrobenzaldehyde	4	6d	25	94	257–259/260–262 <sup>113</sup>
15	Benzaldehyde	4	6e	25	91	258–260/262–264 <sup>111</sup>
16	Terephthaldehyde	4	6f	20	86	297–299/305–307 <sup>114</sup>
17	4-Methylbenzaldehyde	4	6g	25	91	253–255/253–255 <sup>73</sup>
18	3-Methylbenzaldehyde	4	6h	20	89	253–255/250–252 <sup>55</sup>
19	4-Methoxybenzaldehyde	4	6i	35	93	233–235/232–234 <sup>110</sup>
20	Thiophen-2-carbaldehyde	4	6j	35	89	223–225/227–229 <sup>110</sup>

**Table 2.** Three-component synthesis of different 2-amino-7-methyl-5-oxo-4-phenyl-4,5-dihydropyrano[4,3-b]pyran-3-carbonitrile (5a-j) and 2-amino-5-oxo-4-phenyl-4,5-dihydropyrano[3,2-c]chromene-3-carbonitrile (6a-j) via condensation of various aldehydes (1), malononitrile (2) and 4-hydroxy-6-methyl-2H-pyran-2-one (3) or 4-hydroxy coumarin (4) in the presence of MNPs-GO-CysA<sup>a</sup>.



<sup>a</sup>Reaction conditions: Aldehyde (1, 1 mmol), Malononitrile (2, 1.1 mmol), 4-hydroxy-6-methyl-2H-pyran-2-one (3) /or 4-hydroxy coumarin (4) (1 mmol), and MNPs-GO-CysA (15 mg) at reflux conditions. <sup>b</sup>All compounds are known and their structures were established from their melting points as compared with authentic samples or literature values. <sup>c</sup>Isolated yield.

Finally, to demonstrate the effectiveness and efficiency of this new method, the optimized conditions were developed for four-component one-pot condensation of ethyl acetate, hydrazine hydrate/or phenyl hydrazine, malononitrile, and isatin. It should be pointed out that the reaction proceeded at reflux conditions to give the purely expected 6'-amino-3'-methyl-2-oxo-1'H-spiro[indoline-3,4'-pyrano[2,3-c]pyrazole]-5'-carbonitrile (**11a-l**) in quantitative yields in very short reaction time (Table 4).

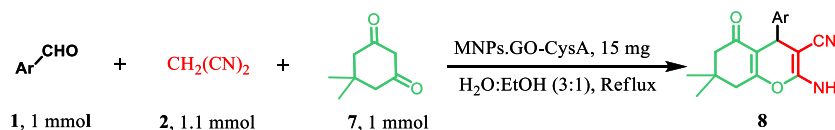
In all studies, the reaction catalyst was simply separated from the main product employing an external magnet after cooling the mixture to r.t. and the precipitated product was filtered out of the reaction mixture.

Due to the importance of using heterogeneous catalysts in industrial processes, we studied the recyclability of the MNPs-GO-CysA nano-catalyst by using it in repeatedly five runs reactions for product **11a** under the optimized reaction conditions. After each reaction cycle, the superparamagnetic catalyst was separated by an external magnetic field and washed twice with hot deionized water (5 mL), once with 5 mL ethanol, dried in an oven at 70 °C, and reused in the model reaction. Summarized results in Fig. 9. implied that a significant reduction in catalytic efficiency was not observed after 5 runs. The strong covalence interaction of cysteine with the GO surface could be the reason for the repetitive use of the catalyst in a greater number of catalytic runs with high efficiency. Eventually, the comparison of the results of FT-IR, EDX, and VSM analysis of the recycled catalyst after five cycles revealed that there are no significant structural changes occurred at the nanoparticle surface (Fig. 10).

In order to evaluate the catalytic efficiency of MNPs-GO-CysA nano-catalyst, we compared the advantages of this catalyst with some other previously reported catalysts for the synthesis of 4H-chromenes. The comparison proved that the catalyst possesses higher activity compared to other catalysts (Table 5).

En	Aldehyde	Enolizable compound	Product <sup>b</sup>	Time (min)	Yield <sup>c</sup> (%)	M.P (°C) Obsd./Lit
1	2-Chlorobenzaldehyde	7	<b>8a</b>	15	95	217–219/213–215 <sup>73</sup>
2	3-Nitrobenzaldehyde	7	<b>8b</b>	15	90	210–211/210–212 <sup>55</sup>
3	2-Nitrobenzaldehyde	7	<b>8c</b>	20	95	218–221/220–222 <sup>55</sup>
4	Benzaldehyde	7	<b>8d</b>	10	90	235–237/231–232 <sup>110</sup>
5	4-Methoxybenzaldehyde	7	<b>8e</b>	15	93	212–214/210–212 <sup>112</sup>
6	4-Methoxybenzaldehyde	7	<b>8f</b>	15	91	195–197/200–202 <sup>73</sup>
7	2,4-dichlorobenzaldehyde	7	<b>8g</b>	15	90	221–223/218–220 <sup>115</sup>
8	Terphthaldehyde	7	<b>8h</b>	30	89	208–211
9	Vanillin	7	<b>8i</b>	20	89	240–242/239–241 <sup>73</sup>
10	Thiophen-2-carbaldehyde	7	<b>8j</b>	30	89	219–220/222–224 <sup>116</sup>

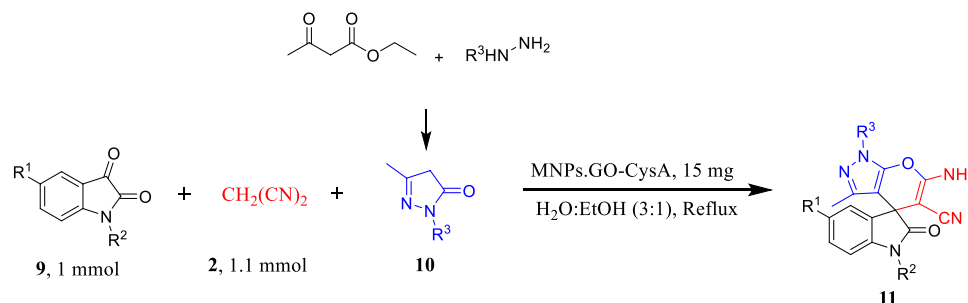
**Table 3.** Three-component synthesis of different 2-amino-7,7-dimethyl-5-oxo-4-aryl-5,6,7,8-tetrahydro-4*H*-chromene-3-carbonitrile (**8a–j**) via condensation of various aldehydes (1), malononitrile (2) and dimedone (7) in the presence of MNPs-GO-CysA<sup>a</sup>.



<sup>a</sup>Reaction conditions: Aldehyde (1, 1 mmol), Malononitrile (2, 1.1 mmol), dimedone (7, 1 mmol), and MNPs-GO-CysA (15 mg) at reflux conditions. <sup>b</sup>All compounds are known and their structures were established from their melting points as compared with authentic samples or literature values. <sup>c</sup>Isolated yield.

En	Isatin	R	Product <sup>b</sup>	Time (min)	Yield <sup>c</sup> (%)	M.P (°C) Obsd./Lit
1	Isatin	H	<b>11a</b>	20	95	269–271/286–287 <sup>67</sup>
2	<i>N</i> -Allyl Isatin	H	<b>11b</b>	25	91	240–242/244–246 <sup>30</sup>
3	<i>N</i> -(4-Nitrobenzyl) Isatin	H	<b>11c</b>	30	88	272–273/271–273 <sup>45</sup>
4	<i>N</i> -Methyl Isatin	H	<b>11d</b>	30	89	261–263/262–264 <sup>30</sup>
5	<i>N</i> -Ethyl Isatin	H	<b>11e</b>	20	90	283–285/285–287 <sup>30</sup>
6	<i>N</i> -Propargyl Isatin	H	<b>11f</b>	25	90	258–259/258–262 <sup>30</sup>
7	<i>N</i> -Benzyl Isatin	H	<b>11g</b>	25	91	232–233/228–232 <sup>30</sup>
8	Isatin	Ph	<b>11h</b>	25	94	223–225/228–230 <sup>41</sup>
9	<i>N</i> -Allyl Isatin	Ph	<b>11i</b>	25	90	213–215/218–220 <sup>117</sup>
10	<i>N</i> -Methyl Isatin	Ph	<b>11j</b>	15	98	226–228/220–222 <sup>118</sup>
11	<i>N</i> -Ethyl Isatin	Ph	<b>11k</b>	20	91	213–215/210–212 <sup>117</sup>
12	<i>N</i> -Benzyl Isatin	Ph	<b>11l</b>	30	89	231–233/228–230 <sup>119</sup>

**Table 4.** Four-component synthesis of different 6'-amino-3'-methyl-2-oxo-1'*H*-spiro[indoline-3,4'-pyrano[2,3-*c*]pyrazole]-5'-carbonitrile (11a-l) via condensation of various isatin (9), malononitrile (2) and 3-methyl-1*H*-pyrazol-5(4*H*)-one (10) in the presence of MNPs-GO-CysA<sup>a</sup>.



<sup>a</sup>Reaction conditions: Isatin (9, 1 mmol), Malononitrile (2, 1.1 mmol), hydrazine compounds (1 mmol), ethyl acetoacetate (1 mmol), and MNPs-GO-CysA (15 mg) at reflux conditions. <sup>b</sup>All compounds are known and their structures were established from their melting points as compared with authentic samples or literature values. <sup>c</sup>Isolated yield.



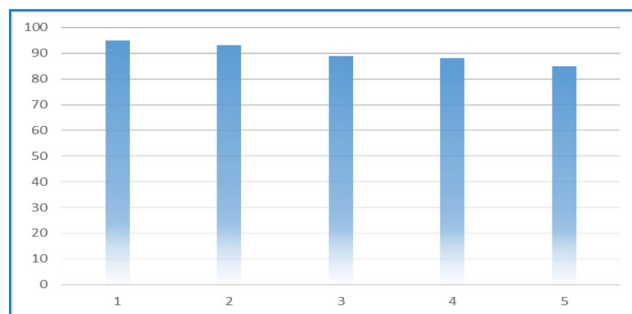


**Figure 9.** The recycling capability of MNPs-GO-CysA nano catalyst in the synthesis of spiro 4*H*-chromene (**11a**) under optimized conditions.

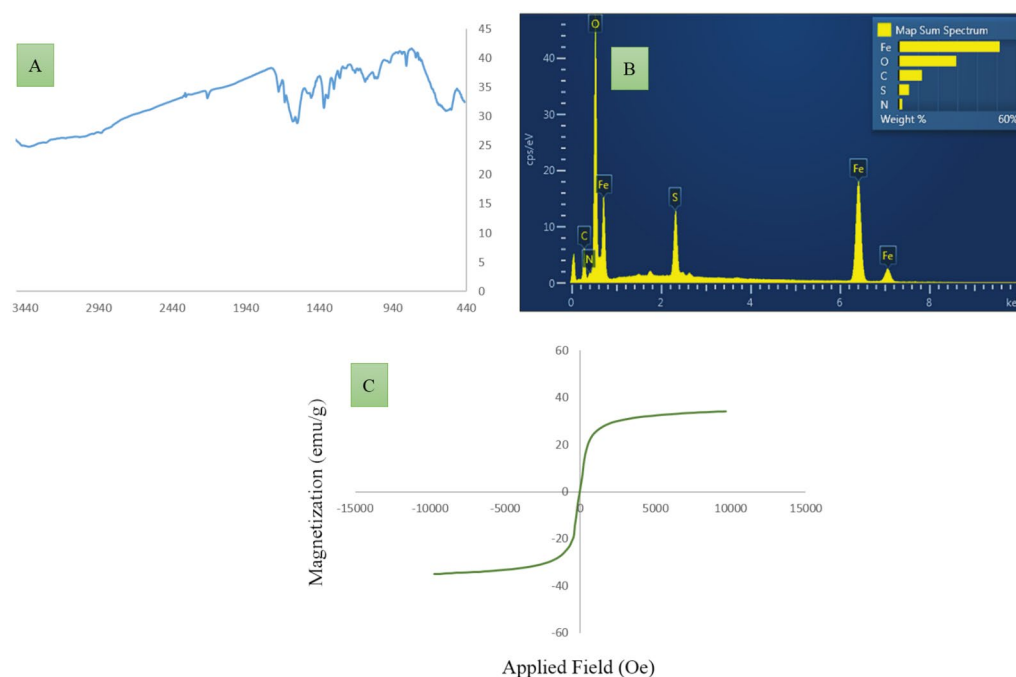


**Figure 10.** The FTIR spectrums (A) and EDX analysis (B) and (C) VSM curve of recovered MNPs-GO-CysA after five runs.

## Conclusions

In summary, we have successfully developed a solid acid supported magnetic graphene oxide catalyzed reaction of an enolizable compound, active methylene nitriles, and aldehydes, which provides rapid and efficient access to different 4*H*-chromene derivatives. Cysteic acid has been incorporated on the magnetic GO successfully and properly dispersed between GO sheets. We have demonstrated that MNPs-GO-CysA acts as a non-hazardous, efficient, reusable, and convenient catalytic system for the synthesis of a wide range of 4*H*-chromenes in water/ethanol as a green solvent. Additionally, the presented catalyst was easily removed from the reaction mixture by means of an external magnet and reused several times with little loss of activity. It can be seen that simplicity in preparation of the present catalyst, efficient recyclability and reusability of the catalyst, short reaction times, and high yields of the products can be considered as outstanding characteristics of the present protocol.

## Experimental

**Materials.** All the materials which were used in our experiments including reagents and solvents were purchased from Merck or Sigma Aldrich. The materials were used without further purification, while benzaldehyde was used freshly after distillation. We used our University's Bruker (Avance DRX-500) spectrometer in order to have our products been checked via  $^1\text{H}$  NMR and  $^{13}\text{C}$  NMR spectrometry using  $\text{CDCl}_3$  as solvent at room temperature. Chemical shifts from the initial standard tetramethylsilane are reported in parts per million (ppm). Using an ABB Bomem MB100 FTIR spectrophotometer, the samples were tested, the results of which are reviewed. CHNS analysis was done by LECO Truspec. Scanning electron microscopy (SEM) was performed on

En	Catalyst	Catalyst loading, Time, Yield, Tem., Solvent	References
1	AcONH <sub>4</sub>	10 mol%, 10 min, 94%, r.t, EtOH	<sup>120a</sup>
2	Piperidine	2 drops, 6 h, 92%, Reflux, EtOH	<sup>59a</sup>
3	MNPs-GO-CysA	15 mg, 30 min, 94%, Reflux, H <sub>2</sub> O:EtOH	This work <sup>a</sup>
4	(2-Aminomethyl)Phenol/ Hydroxyapatite	1.5 mol%, 30 min, 78%, Reflux, H <sub>2</sub> O	<sup>121b</sup>
5	POPINO	5 mol%, 10 min, 97%, Reflux, H <sub>2</sub> O	<sup>51b</sup>
6	Visible Light, 20 W	-, 1.6 h, 87%, -, S-F	<sup>122b</sup>
7	PEI@Si-MNP	5 mg, 55 min, 89%, Reflux, Ethylene Glycol/water	<sup>69b</sup>
8	MNPs-GO-CysA	15 mg, 25 min, 91%, Reflux, H <sub>2</sub> O:EtOH	This work <sup>b</sup>
9	IL-HSO <sub>4</sub> @SBA-15	2 mol%, 2 h, 94%, 45 °C, H <sub>2</sub> O	<sup>42c</sup>
10	Zn <sub>4</sub> O(H <sub>2</sub> N-TA) <sub>3</sub>	40 mg, 5 h, 95%, 60 °C, S-F	<sup>31c</sup>
11	Piperidinium Acetate	10 mol%, 30 min, 92%, r.t, H <sub>2</sub> O	<sup>60c</sup>
12	MNPs-GO-CysA	15 mg, 10 min, 90%, Reflux, H <sub>2</sub> O:EtOH	This work <sup>c</sup>
13	PBBS	20 mg, 4 h, 80%, r.t, CH <sub>3</sub> CN	<sup>75d</sup>
14	Bmim(OH)/ 20 mol% Chitosan	5 ml, 3 h, 92%, r.t, -	<sup>82d</sup>
15	ZnS nanoparticles, Sonicate	10 mol%, 13 min, 96%, r.t, H <sub>2</sub> O	<sup>32d</sup>
16	4-DMAP	10 mol%, 60 min, 83%, 60 °C, EtOH	<sup>58d</sup>
17	Bovine Serum Albumin	60 mg, 30 min, 98%, r.t, H <sub>2</sub> O:EtOH	<sup>84d</sup>
18	MNPs-GO-CysA	15 mg, 20 min, 95%, Reflux, H <sub>2</sub> O:EtOH	This work <sup>d</sup>

**Table 5.** Comparative synthesis of compound **5e**, **6h**, **8d**, and **11h** using the recently reported methods versus the present method. <sup>a</sup>Obtained results for the synthesis of compound **5e**. <sup>b</sup>Obtained results for the synthesis of compound **6h**. <sup>c</sup>Obtained results for the synthesis of compound **8d**. <sup>d</sup>Obtained results for the synthesis of compound **11h**.

VEGA\\TESCAN-LMU. An energy dispersive detector (EDS) coupled to the microscope was used to identify chemical elements of the prepared catalyst. X-ray diffraction (XRD) pattern was recorded on APD 2000 using Cu K $\alpha$  radiation (50 kV, 150 mA) in the range  $2\theta = 10\text{--}120^\circ$ . CHN analysis was done by LECOTruspec.

**Preparation of catalyst.** Graphene oxide (GO) was prepared via a modified Hummers method<sup>123</sup>. The general procedure for preparation of magnetic GO: 50 mL aqueous solution of 4 mmol FeCl<sub>3</sub>·6H<sub>2</sub>O and 2 mmol FeCl<sub>2</sub>·4H<sub>2</sub>O was prepared. The pH of the solution was adjusted to pH = 4 using a NaOH solution (1 M). A Graphene oxide solution was prepared by dispersing 27.5 mg GO in 20 mL water. The Graphene oxide solution was gradually added to the first solution and stirred for 30 min. After that, a sufficient amount of NaOH (1 M) was added to the solution until the pH was adjusted to 10. The reaction was then stirred for 1 h and the resulting precipitate was separated by means of a magnet and washed with DI water and ethanol three times. The resulting precipitate was dried in an oven at 70 °C<sup>124</sup>.

In order to attach L-cysteic acid to the prepared magnetic GO, a mixture of 200 mg of magnetic GO, 50 mg of L-cysteic acid, and 5 ml ethanol was placed in a round bottom flask under stirring for 24 h at room temperature. The obtained precipitate was washed with water and ethanol and dried at 70 °C.

**Synthesis of 4H-chromene derivatives.** A glass vial was successively charged with different enolizable compounds (1 mmol), aldehydes (1 mmol), and active methylene nitrile (1.1 mmol) in the presence of MNPs-GO-CysA (15 mg), in water–ethanol (3:1, 2 mL) at reflux temperature. The reaction mixture was stirred for the appropriate time brought in Tables 2, 3, and 4. After reaction completion, which was controlled by Thin Layer Chromatography (TLC) test (using EtOAc/ n-Hexane, 1:3 as solvent), the catalyst was separated by a magnet, and the obtained solid product was filtered. In the case of impurities, the obtained product was recrystallized from ethanol.

**Synthesis of Spiro 4H-chromene derivatives.** A glass vial was successively charged with hydrazine monohydrate (1.1 mmol), ethyl acetoacetate (1 mmol), MNPs-GO-CysA (15 mg), water–ethanol (3:1, 2 mL) and stirred at reflux conditions for 5 min. Then isatin derivatives (1 mmol), methylene reagent (malononitrile, 1.1 mmol) were added to reaction mixture and stirred for the appropriate time brought in Table 4. After reaction completion, which was controlled by Thin Layer Chromatography (TLC) test (using EtOAc/ n-Hexane, 1:3 as solvent) and the reaction color change from red to white, the catalyst was separated by a magnet, and the obtained solid product was filtered. In the case of impurities, the obtained product was recrystallized from ethanol.

Received: 14 July 2020; Accepted: 17 November 2020

Published online: 01 December 2020

## References

- Sonsona, I. G., Marqués-López, E. & Herrera, R. P. Enantioselective organocatalyzed synthesis of 2-amino-3-cyano-4H-chromene derivatives. *Symmetry* **7**, 1519–1535 (2015).
- Hatakeyama, S., Ochi, N., Numata, H. & Takano, S. A new route to substituted 3-methoxycarbonyldihydropyrans; enantioselective synthesis of (–)-methyl elenolate. *J. Chem. Soc. Chem. Commun.* **17**, 1202–1204 (1988).
- Sturmer, D. M., Weissberger, A. & Taylor, E. C. Syntheses and properties of cyanine and related dyes. In *Special Topics in Heterocyclic Chemistry, Ch. 8, vol. 477* (eds Weissberger, A. & Taylor, E. C.) (Wiley, New York, 1977).
- Shanthia, G., Perumal, P. T., Rao, U. & Sehgal, P. K. Synthesis and antioxidant activity of indolyl chromenes. CSIR, IJC-B Vol.48B (2009).
- Khafagy, M. M., El-Wahas, A., Eid, F. A. & El-Agrody, A. M. Synthesis of halogen derivatives of benzo [h] chromene and benzo [a] anthracene with promising antimicrobial activities. *Farmaco* **57**, 715 (2002).
- Sebahar, P. R. & Williams, R. M. The Asymmetric Total Synthesis of (+)- and (–)-Spirotryprostatin B. *J. Am. Chem. Soc.* **122**, 5666 (2002).
- Kasibhatla, S. *et al.* Discovery and mechanism of action of a novel series of apoptosis inducers with potential vascular targeting activity. *Mol. Cancer Ther.* **3**, 1365–1374 (2004).
- Gourdeau, H. *et al.* Antivascular and antitumor evaluation of 2-amino-4-(3-bromo-4, 5-dimethoxy-phenyl)-3-cyano-4H-chromenes, a novel series of anticancer agents. *Mol. Cancer Ther.* **3**, 1375–1384 (2004).
- Kemnitzner, W. *et al.* Discovery of 4-aryl-4H-chromenes as a new series of apoptosis inducers using a cell- and caspase-based high-throughput screening assay. 2. Structure–activity relationships of the 7- and 5-, 6-, 8-positions. *Bioorgan. Med. Chem. Lett.* **15**, 4745–4751 (2005).
- Skommer, J., Wlodkovic, D., Mättö, M., Eray, M. & Pelkonen, J. HA14-1, a small molecule Bcl-2 antagonist, induces apoptosis and modulates action of selected anticancer drugs in follicular lymphoma B cells. *Leuk. Res.* **30**, 322–331 (2006).
- Cai, S. X. *et al.* (Google Patents, 2011).
- Patil, S. A., Patil, R., Pfeffer, L. M. & Miller, D. D. Chromenes: potential new chemotherapeutic agents for cancer. *Fut. Med. Chem.* **5**, 1647–1660 (2013).
- Evdokimov, N. M. *et al.* Convenient one-step synthesis of a medicinally relevant benzopyranopyridine system. *Tetrahedron Lett.* **47**, 9309–9312 (2006).
- Dell, C. P. & Smith, C. W. European Patent Appl. EP537949. *Chem. Abstr.* **119**, 139102d (1993).
- Szczurowska, E. & Mares, P. Positive allosteric modulator of mGluR4 PHCCC exhibits proconvulsant action in three models of epileptic seizures in immature rats. *Physiol. Res.* **61**, 619 (2012).
- Liu, X. *et al.* The ameliorating effects of 5,7-dihydroxy-6-methoxy-2 (4-phenoxyphenyl)-4H-chromene-4-one, an oroxylin A derivative, against memory impairment and sensorimotor gating deficit in mice. *Arch. Pharmacol. Res.* **36**, 854–863 (2013).
- Konkoy, C. S., Fick, D. B., Cai, S. X., Lan, N. C. & Keana, J. F. W. *Chem. Abstr.* 29313a.
- Kemnitzner, W. *et al.* Discovery of 4-aryl-4H-chromenes as a new series of apoptosis inducers using a cell- and caspase-based high-throughput screening assay. 2. Structure–activity relationships of the 7- and 5-, 6-, 8-positions. *Bioorgan. Med. Chem. Lett.* **15**, 4745–4751 (2005).
- Boominathan, M., Nagaraj, M., Muthusubramanian, S. & Krishnakumar, R. V. Efficient atom economical one-pot multicomponent synthesis of densely functionalized 4H-chromene derivatives. *Tetrahedron* **67**, 6057–6064 (2011).
- Slobbe, P., Ruijter, E. & Orru, R. V. A. Recent applications of multicomponent reactions in medicinal chemistry. *MedChemComm* **3**, 1189–1218 (2012).
- Azizi, N., Mariami, M. & Edrisi, M. Greener construction of 4H-chromenes based dyes in deep eutectic solvent. *Dyes Pigment.* **100**, 215–221 (2014).
- Rotstein, B. H., Zaretsky, S., Rai, V. & Yudin, A. K. Small heterocycles in multicomponent reactions. *Chem. Rev.* **114**, 8323–8359 (2014).
- Biggs-Houck, J. E., Younai, A. & Shaw, J. T. Recent advances in multicomponent reactions for diversity-oriented synthesis. *Curr. Opin. Chem. Biol.* **14**, 371–382 (2010).
- Estevez, V., Villacampa, M. & Menendez, J. C. Recent advances in the synthesis of pyrroles by multicomponent reactions. *Chem. Soc. Rev.* **43**, 4633–4657 (2014).
- Isambert, N. *et al.* Multicomponent reactions and ionic liquids: a perfect synergy for eco-compatible heterocyclic synthesis. *Chem. Soc. Rev.* **40**, 1347–1357 (2011).
- Kumaravel, K. & Vasuki, G. Multicomponent reactions in water. *ChemInform* <https://doi.org/10.1002/chin.201014221> (2010).
- Zarei, A., Yarie, M., Zolfigol, M. A. & Niknam, K. Synthesis of a novel bifunctional oxyammonium-based ionic liquid: Application for the synthesis of pyrano[4,3-b]pyrans and tetrahydrobenzo[b]pyrans. *J. Chin. Chem. Soc.* <https://doi.org/10.1002/jccs.201800468> (2019).
- Eshghi, H., Zohuri, G. H. & Damavandi, S. Highly efficient Fe(HSO<sub>4</sub>)<sub>3</sub>-catalyzed one-pot Mannich-type reactions: three component synthesis of β-amino carbonyl compounds. *Synth. React. Inorg. Met. Org. Nano Met. Chem.* **41**, 266–271 (2011).
- Khurana, J. M. & Vij, K. Nickel nanoparticles as semiheterogeneous catalyst for one-pot, three-component synthesis of 2-amino-4H-pyrans and pyran annulated heterocyclic moieties. *Synth. Commun.* **43**, 2294–2304 (2013).
- Bodhak, C., Kundu, A. & Pramanik, A. ZrO<sub>2</sub> nanoparticles as a reusable solid dual acid–base catalyst for facile one-pot synthesis of multi-functionalized spirooxindole derivatives under solvent free condition. *RSC Adv.* **5**, 85202–85213 (2015).
- Rostamnia, S. & Morsali, A. Size-controlled crystalline basic nanoporous coordination polymers of Zn<sub>4</sub>O(H<sub>2</sub>N-TA)<sub>3</sub>: catalytic study of IRMOF-3 as a suitable and green catalyst for selective synthesis of tetrahydro-chromenes. *Inorg. Chim. Acta* **411**, 113–118 (2014).
- Dandia, A., Parewa, V., Jain, A. K. & Rathore, K. S. Step-economic, efficient, ZnS nanoparticle-catalyzed synthesis of spirooxindole derivatives in aqueous medium via Knoevenagel condensation followed by Michael addition. *Green Chem.* **13**, 2135–2145 (2011).
- Kumar, D. *et al.* Nanosized magnesium oxide as catalyst for the rapid and green synthesis of substituted 2-amino-2-chromenes. *Tetrahedron* **63**, 3093–3097 (2007).
- Rajput, J. K. & Kaur, G. Synthesis and applications of CoFe<sub>2</sub>O<sub>4</sub> nanoparticles for multicomponent reactions. *Catal. Sci. Technol.* **4**, 142–151 (2014).
- Albadi, J., Razeghi, A., Mansournezhad, A. & Azarian, Z. CuO–CeO<sub>2</sub> nanocomposite catalyzed efficient synthesis of amino-chromenes. *J. Nanostruct. Chem.* **3**, 85 (2013).
- Mosaddegh, E. Ultrasonic-assisted preparation of nano eggshell powder: A novel catalyst in green and high efficient synthesis of 2-aminochromenes. *Ultrason. Sonochem.* **20**, 1436–1441 (2013).
- Al-Matar, H. M., Khalil, K. D., Meier, H., Kolshorn, H. & Elnagdi, M. H. Chitosan as heterogeneous catalyst in Michael additions: the reaction of cinnamionitriles with active methylene moieties and phenols. *Arkivoc* **16**, 288–301 (2008).
- Hershberger, J. C., Zhang, L., Lu, G. & Malinakova, H. C. Polymer-supported palladacycles: Efficient reagents for synthesis of Benzopyrans with palladium recovery Relationship among resin loading, Pd: P ratio, and reactivity of immobilized palladacycles. *J. Organ. Chem.* **71**, 231–235 (2006).

39. Peng, Y. & Song, G. Amino-functionalized ionic liquid as catalytically active solvent for microwave-assisted synthesis of 4H-pyrans. *Catal. Commun.* **8**, 111–114 (2007).
40. Zhou, J. F., Tu, S. J., Gao, Y. & Ji, M. C. Synthesis and reaction of some new 4H-pyrano [3, 2-c] benzopyran-5-one derivatives and their potential biological activity. *J. Org. Chem.* **21**, 742–744 (2001).
41. Padvi, S. A., Tayade, Y. A., Wagh, Y. B. & Dalal, D. S. [bmim]OH: An efficient catalyst for the synthesis of mono and bis spirooxindole derivatives in ethanol at room temperature. *Chin. Chem. Lett.* **27**, 714–720 (2016).
42. Rostamnia, S., Hassankhani, A., Hossieni, H. G., Gholipour, B. & Xin, H. Brønsted acidic hydrogensulfate ionic liquid immobilized SBA-15:[MPIm][HSO<sub>4</sub>]@ SBA-15 as an environmentally friendly, metal-and halogen-free recyclable catalyst for Knoevenagel–Michael-cyclization processes. *J. Mol. Catal. A: Chem.* **395**, 463–469 (2014).
43. Jin, T.-S., Wang, A.-Q., Wang, X., Zhang, J.-S. & Li, T.-S. A clean one-pot synthesis of tetrahydrobenzo [b] pyran derivatives catalyzed by hexadecyltrimethyl ammonium bromide in aqueous media. *Synlett* **2004**, 0871–0873 (2004).
44. Balalaie, S., Bararjanian, M., Amani, A. M. & Movassagh, B. (S)-Proline as a neutral and efficient catalyst for the one-pot synthesis of tetrahydrobenzo [b] pyran derivatives in aqueous media. *Synlett* **2006**, 263–266 (2006).
45. Nagaraju, S., Paplal, B., Sathish, K., Giri, S. & Kashinath, D. Synthesis of functionalized chromene and spirochromenes using L-proline-melamine as highly efficient and recyclable homogeneous catalyst at room temperature. *Tetrahedron Lett.* **58**, 4200–4204 (2017).
46. Gao, S., Tsai, C. H., Tseng, C. & Yao, C.-F. Fluoride ion catalyzed multicomponent reactions for efficient synthesis of 4H-chromene and N-arylquinoline derivatives in aqueous media. *Tetrahedron* **64**, 9143–9149 (2008).
47. Jin, T. S., Zhang, J. S., Liu, L. B., Wang, A. Q. & Li, T. S. Clean, One-Pot Synthesis of Naphthopyran Derivatives in Aqueous Media. *Synth. Commun.* **36**, 2009–2015 (2006).
48. Chen, L., Huang, X.-J., Li, Y.-Q., Zhou, M.-Y. & Zheng, W.-J. A one-pot multicomponent reaction for the synthesis of 2-amino-2-chromenes promoted by N,N-dimethylamino-functionalized basic ionic liquid catalysis under solvent-free condition. *Monatshfte für Chemie-Chemical Monthly* **140**, 45 (2009).
49. Hasaninejad, A., Shekouhy, M., Golzar, N., Zare, A. & Doroodmand, M. M. Silica bonded n-propyl-4-aza-1-azoniabicyclo [2.2.2] octane chloride (SB-DABCO): A highly efficient, reusable and new heterogeneous catalyst for the synthesis of 4H-benzo [b] pyran derivatives. *Applied Catalysis A: General* **402**, 11–22 (2011).
50. Hasaninejad, A., Golzar, N., Beyrati, M., Zare, A. & Doroodmand, M. M. Silica-bonded 5-n-propyl-octahydro-pyrimido[1,2-a] azeponium chloride (SB-DBU)Cl as a highly efficient, heterogeneous and recyclable silica-supported ionic liquid catalyst for the synthesis of benzo[b]pyran, bis(benzo[b]pyran) and spiro-pyran derivatives. *J. Mol. Catal. A: Chem.* **372**, 137–150 (2013).
51. Dekamin, M. G., Eslami, M. & Maleki, A. Potassium phthalimide-N-oxyl: a novel, efficient, and simple organocatalyst for the one-pot three-component synthesis of various 2-amino-4H-chromene derivatives in water. *Tetrahedron* **69**, 1074–1085 (2013).
52. Dekamin, M. G. & Eslami, M. Highly efficient organocatalytic synthesis of diverse and densely functionalized 2-amino-3-cyano-4H-pyrans under mechanochemical ball milling. *Green Chem.* **16**, 4914–4921 (2014).
53. Hekmatshoar, R., Majedi, S. & Bakhtiari, K. Sodium selenate catalyzed simple and efficient synthesis of tetrahydro benzo [b] pyran derivatives. *Catal. Commun.* **9**, 307–310 (2008).
54. Dekamin, M. G. *et al.* Sodium alginate: an efficient biopolymeric catalyst for green synthesis of 2-amino-4H-pyran derivatives. *Int. J. Biol. Macromol.* **87**, 172–179 (2016).
55. Chen, L., Lin, J., Chen, B. & Zhao, L. Sodium ethylene diamine tetraacetate catalyzed synthesis of chromene derivatives via multi-component reactions at low catalyst loading. *Res. Chem. Intermed.* **43**, 6691–6700 (2017).
56. Heravi, M. M., Zakeri, M. & Mohammadi, N. Guanidine hydrochloride: An active and simple catalyst for Mannich type reaction in solvent-free condition. *Chin. Chem. Lett.* **22**, 797–800 (2011).
57. Khan, A. T., Lal, M., Ali, S. & Khan, M. M. One-pot three-component reaction for the synthesis of pyran annulated heterocyclic compounds using DMAP as a catalyst. *Tetrahedron Lett.* **52**, 5327–5332 (2011).
58. Feng, J., Ablajan, K. & Sali, A. 4-Dimethylaminopyridine-catalyzed multi-component one-pot reactions for the convenient synthesis of spiro[indoline-3,4'-pyrano[2,3-c]pyrazole] derivatives. *Tetrahedron* **70**, 484–489 (2014).
59. Stoyanov, E. V., Ivanov, I. C. & Heber, D. General method for the preparation of substituted 2-amino-4H, 5H-pyrano[4,3-b] pyran-5-ones and 2-amino-4H-pyrano[3,2-c]pyridine-5-ones. *Molecules* **5**, 19–32 (2000).
60. Indrasena, A., Riyaz, S., Naidu, A. & Dubey, P. A facile, eco-friendly, proton donor-acceptor catalyzed, one-pot, three-component synthesis of tetrahydrobenzo [b] pyrans. *Asian J. Chem.* **26**, 2221 (2014).
61. Xie, J., Xing, X.-Y., Sha, F., Wu, Z.-Y. & Wu, X.-Y. Enantioselective synthesis of spiro[indoline-3,4[prime or minute]-pyrano[2,3-c] pyrazole] derivatives via an organocatalytic asymmetric Michael/cyclization cascade reaction. *Org. Biomol. Chem.* **14**, 8346–8355 (2016).
62. Kundu, S. K., Mondal, J. & Bhaumik, A. Tungstic acid functionalized mesoporous SBA-15: A novel heterogeneous catalyst for facile one-pot synthesis of 2-amino-4H-chromenes in aqueous medium. *Dalton Trans.* **42**, 10515–10524 (2013).
63. Khurana, J. M., Nand, B. & Saluja, P. DBU: a highly efficient catalyst for one-pot synthesis of substituted 3,4-dihydropyrano[3,2-c] chromenes, dihydropyrano[4,3-b]pyranes, 2-amino-4H-benzo [h] chromenes and 2-amino-4H-benzo [g] chromenes in aqueous medium. *Tetrahedron* **66**, 5637–5641 (2010).
64. Patil, D. *et al.* Novel Brønsted acidic ionic liquid ([CMIM][CF<sub>3</sub>COO]) prompted multicomponent hantzsch reaction for the eco-friendly synthesis of acridinediones: an efficient and recyclable catalyst. *Catal. Lett.* **144**, 949–958 (2014).
65. Khan, M. N., Pal, S., Karamthulla, S. & Choudhury, L. H. Imidazole as organocatalyst for multicomponent reactions: Diversity oriented synthesis of functionalized hetero- and carbocycles using in situ-generated benzylidenemalononitrile derivatives. *RSC Adv.* **4**, 3732–3741 (2014).
66. Heravi, M. M., Bakhtiari, K., Zadsirjan, V., Bamoharram, F. F. & Heravi, O. M. Aqua mediated synthesis of substituted 2-amino-4H-chromenes catalyzed by green and reusable Preysslter heteropolyacid. *Bioorg. Med. Chem. Lett.* **17**, 4262–4265 (2007).
67. Guo, R.-Y. *et al.* Meglumine: A novel and efficient catalyst for one-pot, three-component combinatorial synthesis of functionalized 2-amino-4H-pyrans. *ACS Combin. Sci.* **15**, 557–563 (2013).
68. Kale, S. R., Kahandal, S. S., Burange, A. S., Gawande, M. B. & Jayaram, R. V. A benign synthesis of 2-amino-4H-chromene in aqueous medium using hydrotalcite (HT) as a heterogeneous base catalyst. *Catal. Sci. Technol.* **3**, 2050–2056 (2013).
69. Hamadi, H., Gholami, M. & Khoobi, M. Polyethyleneimine-modified super paramagnetic Fe<sub>3</sub>O<sub>4</sub> nanoparticles: an efficient, reusable and water tolerance nanocatalyst. *Int. J. Heterocycl. Chem.* **1**(3), 23–34 (2011).
70. Shitole, N. V., Shelke, K. F., Sadaphal, S. A., Shingate, B. B. & Shingare, M. S. PEG-400 remarkably efficient and recyclable media for one-pot synthesis of various 2-amino-4H-chromenes. *Green Chem. Lett. Rev.* **3**, 83–87 (2010).
71. Maggi, R., Ballini, R., Sartori, G. & Sartorio, R. Basic alumina catalysed synthesis of substituted 2-amino-2-chromenes via three-component reaction. *Tetrahedron Lett.* **45**, 2297–2299 (2004).
72. Baghbanian, S. M., Rezaei, N. & Tashakkorian, H. Nanozeolite clinoptilolite as a highly efficient heterogeneous catalyst for the synthesis of various 2-amino-4H-chromene derivatives in aqueous media. *Green Chem.* **15**, 3446–3458 (2013).
73. Abbaspour-Gilandeh, E., Aghaei-Hashjin, M., Yahyazadeh, A. & Salemi, H. (CTA)<sub>3</sub>[SiW<sub>12</sub>]-Li+-MMT: A novel, efficient and simple nanocatalyst for facile and one-pot access to diverse and densely functionalized 2-amino-4H-chromene derivatives via an eco-friendly multicomponent reaction in water. *RSC Adv.* **6**, 55444–55462 (2016).

74. Yaghoobi, A., Dekamin, M. G., Arefi, E. & Karimi, B. Propylsulfonic acid-anchored isocyanurate-based periodic mesoporous organosilica (PMO-ICS-Pr-SO<sub>3</sub>H): A new and highly efficient recoverable nanoporous catalyst for the one-pot synthesis of bis (indolyl) methane derivatives. *J. Colloid Interface Sci.* **505**, 956–963 (2017).
75. Ghorbani-Vaghei, R. & Malaekhepoor, S. M. N-Bromosulfonamides catalyzed synthesis of new spiro[indoline-3,4'-pyrano [2,3-c] pyrazole] derivatives. *J. Heterocycl. Chem.* **54**, 465–472 (2017).
76. Ballini, R. *et al.* Multicomponent reactions under clay catalysis. *Catal. Today* **60**, 305–309 (2000).
77. Elinson, M. N. *et al.* Solvent-free cascade reaction: direct multicomponent assembling of 2-amino-4H-chromene scaffold from salicylaldehyde, malononitrile or cyanoacetate and nitroalkanes. *Tetrahedron* **66**, 4043–4048 (2010).
78. Heravi, M. M., Baghernejad, B. & Oskooie, H. A. A novel and efficient catalyst to one-pot synthesis of 2-amino-4H-chromenes by methanesulfonic acid. *J. Chin. Chem. Soc.* **55**, 659–662 (2008).
79. Sunil Kumar, B. *et al.* An efficient approach towards three component coupling of one pot reaction for synthesis of functionalized benzopyrans. *J. Heterocycl. Chem.* **43**, 1691–1693 (2006).
80. Eshghi, H., Damavandi, S. & Zohuri, G. H. Efficient One-Pot Synthesis of 2-Amino-4H-chromenes Catalyzed by Ferric Hydrogen Sulfate and Zr-Based Catalysts of FI. *Synth. React. Inorg. Nano-Met. Chem.* **41**(9), 1067–1073 (2011).
81. Mohire, P. P. *et al.* Protic ionic liquid promoted one pot synthesis of 2-amino-4-(phenyl)-7-methyl-5-oxo-4H, 5H-pyrano[4,3-b] pyran-3-carbonitrile derivatives in water and their antimycobacterial activity. *J. Heterocycl. Chem.* **55**, 1010–1023 (2018).
82. Rai, P., Srivastava, M., Singh, J. & Singh, J. Chitosan/ionic liquid forms a renewable and reusable catalyst system used for the synthesis of highly functionalized spiro derivatives. *New J. Chem.* **38**, 3181–3186 (2014).
83. Yi, F., Peng, Y. & Song, G. Microwave-assisted liquid-phase synthesis of methyl 6-amino-5-cyano-4-aryl-2-methyl-4H-pyran-3-carboxylate using functional ionic liquid as soluble support. *Tetrahedron Lett.* **46**, 3931–3933 (2005).
84. Dalal, K. S. *et al.* Bovine serum albumin catalyzed one-pot, three-component synthesis of dihydropyrano[2,3-c]pyrazole derivatives in aqueous ethanol. *RSC Adv.* **6**, 14868–14879 (2016).
85. Kumar, D., Reddy, V. B., Sharad, S., Dube, U. & Kapur, S. A facile one-pot green synthesis and antibacterial activity of 2-amino-4H-pyrans and 2-amino-5-oxo-5,6,7,8-tetrahydro-4H-chromenes. *Eur. J. Med. Chem.* **44**, 3805–3809 (2009).
86. Wang, D. & Astruc, D. Fast-growing field of magnetically recyclable nanocatalysts. *Chem. Rev.* **114**, 6949–6985 (2014).
87. Yuan, X., Wang, Z., Zhang, Q. & Luo, J. An intramolecular relay catalysis strategy for Knoevenagel condensation and 1,3-dipolar cycloaddition domino reactions. *RSC Adv.* **9**, 23614–23621 (2019).
88. Rossi, L. M., Costa, N. J., Silva, F. P. & Wojcieszak, R. Magnetic nanomaterials in catalysis: Advanced catalysts for magnetic separation and beyond. *Green Chem.* **16**, 2906–2933 (2014).
89. Mohammad Ali, B., Mahdia, H. & Najmieh, A. Recent advances in the preparation and application of organic–inorganic hybrid magnetic nanocatalysts on multicomponent reactions. *Curr. Organ. Chem.* **22**, 234–267 (2018).
90. Ahadi, N., Bodaghifard, M. A. & Mobinikhaledi, A. Cu(II)- $\beta$ -cyclodextrin complex stabilized on magnetic nanoparticles: A retrievable hybrid promoter for green synthesis of spiroyrans. *Appl. Organomet. Chem.* **33**, e4738 (2019).
91. Gao, W. The chemistry of graphene oxide. In *Graphene Oxide: Reduction Recipes, Spectroscopy, and Applications* (ed. Gao, W.) 61–95 (Springer, Berlin, 2015).
92. Safari, J., Gandomi-Ravandi, S. & Ashiri, S. Organosilane sulfonated graphene oxide in the Biginelli and Biginelli-like reactions. *New J. Chem.* **40**, 512–520 (2016).
93. Wang, C. *et al.* Direct hydroxylation of benzene to phenol over metal oxide supported graphene oxide catalysts. *Catal. Commun.* **68**, 1–5 (2015).
94. Kim, J. *et al.* Graphene oxide sheets at interfaces. *J. Am. Chem. Soc.* **132**, 8180–8186 (2010).
95. Suk, J. W., Piner, R. D., An, J. & Ruoff, R. S. Mechanical properties of monolayer graphene oxide. *ACS Nano* **4**, 6557–6564 (2010).
96. Akbari, M., Shariaty-Niassar, M., Matsuura, T. & Ismail, A. F. Janus graphene oxide nanosheet: A promising additive for enhancement of polymeric membranes performance prepared via phase inversion. *J. Colloid Interface Sci.* **527**, 10–24 (2018).
97. Sobhani, S., Zarifi, F. & Skibsted, J. Ionic liquids grafted onto graphene oxide as a new multifunctional heterogeneous catalyst and its application in the one-pot multi-component synthesis of hexahydroquinolines. *New J. Chem.* **41**, 6219–6225 (2017).
98. Seyedi, N., Saidi, K. & Sheibani, H. Green synthesis of Pd nanoparticles supported on magnetic graphene oxide by *Origanum vulgare* leaf plant extract: Catalytic activity in the reduction of organic dyes and Suzuki-Miyaura cross-coupling reaction. *Catal. Lett.* **148**, 277–288 (2017).
99. Paredes, J., Villar-Rodil, S., Martínez-Alonso, A. & Tascon, J. Graphene oxide dispersions in organic solvents. *Langmuir* **24**, 10560–10564 (2008).
100. Liu, S., Wang, H., Chai, L. & Li, M. Effects of single- and multi-organic acid ligands on adsorption of copper by Fe<sub>3</sub>O<sub>4</sub>/graphene oxide-supported DCTA. *J. Colloid Interface Sci.* **478**, 288–295 (2016).
101. Pérez-Quintanilla, D., Morante-Zarcelo, S. & Sierra, I. Preparation and characterization of mesoporous silicas modified with chiral selectors as stationary phase for high-performance liquid chromatography. *J. Colloid Interface Sci.* **414**, 14–23 (2014).
102. Hu, X.-J. *et al.* Effect of aniline on cadmium adsorption by sulfanilic acid-grafted magnetic graphene oxide sheets. *J. Colloid Interface Sci.* **426**, 213–220 (2014).
103. Yang, S.-T. *et al.* Folding/aggregation of graphene oxide and its application in Cu<sup>2+</sup> removal. *J. Colloid Interface Sci.* **351**, 122–127 (2010).
104. Hu, X.-J. *et al.* Effects of background electrolytes and ionic strength on enrichment of Cd(II) ions with magnetic graphene oxide-supported sulfanilic acid. *J. Colloid Interface Sci.* **435**, 138–144 (2014).
105. Rajabi-Salek, M., Zolfigol, M. A. & Zarei, M. Synthesis of a novel DABCO-based nanomagnetic catalyst with sulfonic acid tags: application to the synthesis of diverse spiroyrans. *Res. Chem. Intermed.* **44**, 5255–5269 (2018).
106. Bodaghifard, M., Mobinikhaledi, A. & Asadbegi, S. Bis(4-pyridylamino) triazine-stabilized magnetite nanoparticles: preparation, characterization and application as a retrievable catalyst for the green synthesis of 4H-pyran, 4H-thiopyran and 1,4-dihydropyridine derivatives. *Appl. Organomet. Chem.* **31**, e3557 (2017).
107. Bonyasi, F., Hekmati, M. & Veisi, H. Preparation of core/shell nanostructure Fe<sub>3</sub>O<sub>4</sub>@PEG400-SO<sub>3</sub>H as heterogeneous and magnetically recyclable nanocatalyst for one-pot synthesis of substituted pyrroles by Paal–Knorr reaction at room temperature. *J. Colloid Interface Sci.* **496**, 177–187 (2017).
108. Doustkhah, E. & Rostamnia, S. Covalently bonded sulfonic acid magnetic graphene oxide: Fe<sub>3</sub>O<sub>4</sub>@GO-Pr-SO<sub>3</sub>H as a powerful hybrid catalyst for synthesis of indazolophthalazinetriones. *J. Colloid Interface Sci.* **478**, 280–287 (2016).
109. Nersasian, A. & Johnson, P. R. Infrared spectra of alkanesulfonic acids, chlorosulfonated polyethylene, and their derivatives. *J. Appl. Polym. Sci.* **9**, 1653–1668 (1965).
110. Abaszadeh, M. & Seifi, M. Crown ether complex cation ionic liquids (CECILs) as environmentally benign catalysts for three-component synthesis of 4,5-dihydropyrano[3,2-c]chromene and 4,5-dihydropyrano[4,3-b]pyran derivatives. *Res. Chem. Intermed.* **41**, 7715–7723 (2015).
111. Karami, B., Kiani, M., Hosseini, S. J. & Bahrami, M. Synthesis and characterization of novel nanosilica molybdenic acid and its first catalytic application in the synthesis of new and known pyranocoumarins. *New J. Chem.* **39**, 8576–8581 (2015).
112. Hazeri, N. *et al.* An efficient one-pot three-component synthesis of tetrahydrobenzo[b]pyran and 3,4-dihydropyrano[c]chromene derivatives using starch solution as catalyst. *Chin. J. Catal.* **35**, 391–395 (2014).
113. Kangani, M., Hazeri, N. & Maghsoodlou, M. T. A Mild and Environmentally Benign Synthesis of Tetrahydrobenzo [b] pyrans and Pyrano [c] chromenes Using Pectin as a Green and Biodegradable Catalyst. *J. Chin. Chem. Soc.* **63**, 896–901 (2016).

114. Goli-Jolodar, O., Shirini, F. & Seddighi, M. An efficient and practical synthesis of specially 2-amino-4H-pyrans catalyzed by C4(DABCO-SO3H)2·4Cl. *Dyes Pigm.* **133**, 292–303 (2016).
115. Zolfigol, M. A., Bahrami-Nejad, N., Afsharnadery, F. & Bagheri, S. 1-Methylimidazolium tricyanomethanide [HMIM]C(CN)<sub>3</sub> as a nano structure and reusable molten salt catalyst for the synthesis of tetrahydrobenzo[b]pyrans via tandem Knoevenagel–Michael cyclocondensation and 3,4-dihydropyrano[c]chromene derivatives. *J. Mol. Liq.* **221**, 851–859 (2016).
116. Dekamin, M. G. & Eslami, M. Highly efficient organocatalytic synthesis of diverse and densely functionalized 2-amino-3-cyano-4H-pyrans under mechanochemical ball milling. *Green Chem.* **16**, 4914–4921 (2014).
117. Dandia, A., Saini, D., Bhaskaran, S. & Saini, D. K. Ultrasound promoted green synthesis of spiro [pyrano[2,3-c]pyrazoles] as antioxidant agents. *Med. Chem. Res.* **23**, 725–734 (2014).
118. Heravi, M. M., Hashemi, E. & Azimian, F. N-Sulfonic acid modified poly (styrene-co-maleic anhydride): An efficient and recyclable solid acid catalyst for the synthesis of a wide range of spiroopyrans. *J. Iran. Chem. Soc.* **12**, 647–653 (2015).
119. Khazaei, A., Zolfigol, M. A., Karimitabar, F., Nikokar, I. & Moosavi-Zare, A. R. N,2-Dibromo-6-chloro-3,4-dihydro-2H-benzo[e][1,2,4]thiadiazine-7-sulfonamide 1,1-dioxide: an efficient and homogeneous catalyst for one-pot synthesis of 4H-pyran, pyranopyrazole and pyrazolo [1,2-b] phthalazine derivatives under aqueous media. *RSC Advances* **5**, 71402–71412 (2015).
120. Rajguru, D., Keshwal, B. S. & Jain, S. Solvent-free, green and efficient synthesis of pyrano [4,3-b] pyrans by grinding and their biological evaluation as antitumor and antioxidant agents. *Med. Chem. Res.* **22**, 5934–5939 (2013).
121. Khoobi, M. *et al.* Design, synthesis, docking study and biological evaluation of some novel tetrahydrochromeno [3',4':5,6] pyrano[2,3-b] quinolin-6(7H)-one derivatives against acetyl- and butyrylcholinesterase. *Eur. J. Med. Chem.* **68**, 291–300 (2013).
122. Tiwari, J. *et al.* Visible light promoted synthesis of dihydropyrano[2,3-c]chromenes via a multicomponent-tandem strategy under solvent and catalyst free conditions. *Green Chem.* **18**, 3221–3231 (2016).
123. Hummers, W. S. Jr. & Offeman, R. E. Preparation of graphitic oxide. *J. Am. Chem. Soc.* **80**, 1339–1339 (1958).
124. Zubir, N. A., Yacou, C., Motuzas, J., Zhang, X. & Da Costa, J. C. D. Structural and functional investigation of graphene oxide-Fe<sub>3</sub>O<sub>4</sub> nanocomposites for the heterogeneous Fenton-like reaction. *Sci. Rep.* **4**, 4594 (2014).

## Acknowledgements

We gratefully acknowledge the funding support received for this project from the Sharif University of Technology (SUT), Islamic Republic of Iran.

## Author contributions

M.E. worked on the topic as his Ph.D. thesis and prepared the initial draft of the manuscript. Dr. F.M.M. is the supervisor of M.E. as his Ph.D. student. Also, he edited and revised the manuscript completely. G.H. worked closely with M.E. for doing the experimental section.

## Competing interests

The authors declare no competing interests.

## Additional information

**Supplementary information** is available for this paper at <https://doi.org/10.1038/s41598-020-77872-8>.

**Correspondence** and requests for materials should be addressed to F.M.M.

**Reprints and permissions information** is available at [www.nature.com/reprints](http://www.nature.com/reprints).

**Publisher's note** Springer Nature remains neutral with regard to jurisdictional claims in published maps and institutional affiliations.



**Open Access** This article is licensed under a Creative Commons Attribution 4.0 International License, which permits use, sharing, adaptation, distribution and reproduction in any medium or format, as long as you give appropriate credit to the original author(s) and the source, provide a link to the Creative Commons licence, and indicate if changes were made. The images or other third party material in this article are included in the article's Creative Commons licence, unless indicated otherwise in a credit line to the material. If material is not included in the article's Creative Commons licence and your intended use is not permitted by statutory regulation or exceeds the permitted use, you will need to obtain permission directly from the copyright holder. To view a copy of this licence, visit <http://creativecommons.org/licenses/by/4.0/>.

© The Author(s) 2020